IIETA International Information and Engineering Technology Association
Advancing the World of Information and Engineering

Annales de Chimie - Science des Matériaux
Vol. 50, No. 3, June, 2026, pp. 303-315
Journal homepage: http://iieta.org/journals/acsm

Mechanical, Tribological, and Cytocompatibility Evaluation of Nano-Hydroxyapatite/UHMWPE Fiber-Reinforced Hybrid Composites with Plasma Immersion Ion Implantation Surface Treatment

Yahya Ali Jasim*, Asra Ali Hussein

Department of Polymer and Petrochemical Industries, College of Materials Engineering, University of Babylon, Babylon 51001, Iraq

Corresponding Author Email: mat321.yahya.ali@student.uobabylon.edu.iq

https://doi.org/10.18280/acsm.500310

Received: 8 April 2026
Revised: 2 June 2026
Accepted: 10 June 2026
Available online: 30 June 2026

Keywords:
ultra-high molecular weight polyethylene, nano-hydroxyapatite, hybrid polymer composites, tribological behavior, wear resistance, cytocompatibility

ABSTRACT

Ultra-high molecular weight polyethylene (UHMWPE) is widely used in biomedical and orthopedic applications because of its chemical stability, low friction, and generally favorable biological response. Even so, wear and mechanical stability can remain limiting factors under repeated loading. In this work, UHMWPE composites containing 40 wt.% UHMWPE fibers were prepared with 1–3 wt.% nano-hydroxyapatite (nHAp) by thermo-compression molding. Their mechanical, thermal, morphological, tribological, and in vitro cytocompatibility responses were then examined. As the nHAp content increased, the average density rose from 0.9496 to 0.9755 g/cm³, Shore D hardness from 62 to 62.9, and impact strength from 0.0515 to 0.055 J/mm². Among the tested compositions, the 3 wt.% nHAp sample gave the highest average bending-related values. Flexural strength changed from 21.6 MPa in the fiber-only composite to 39 MPa, while flexural modulus increased from 0.592 to 1.954 GPa. Its tensile strength was 117 MPa, compared with 121 MPa for the composite without nHAp. Under dry sliding, the average friction coefficient decreased from 0.20 to 0.144 after nHAp addition, and the wear coefficient changed from 4.45×10^{-4} to 2.20×10^{-4}. After plasma immersion ion implantation (PIII) treatment, the friction and wear values decreased only slightly, reaching 0.138 and 2.17×10^{-4}, respectively. Both human dermal fibroblast cells (HdFn) and Mg-63 cells retained a viability above 90%. Overall, the selected composite showed a combination of mechanical, dry-sliding, and initial in vitro responses under the conditions examined in this study.

1. INTRODUCTION

Polymer composites are used in engineering and biomedical fields because they can give low-weight materials with useful mechanical and wear properties [1]. Ultra-high molecular weight polyethylene (UHMWPE) is used in many biomedical parts because it is chemically stable and has low friction. It also shows good biological acceptance in contact with body tissues [2]. However, UHMWPE can still have wear problems and may lose part of its mechanical stability under repeated loading [3]. Consequently, extensive research has been carried out to improve the mechanical and tribological characteristics of UHMWPE-based composites by incorporating reinforcing materials [4]. Fiber reinforcement has been considered to be one of the most effective methods to improve the mechanical strength and stiffness of the matrix. In this context, UHMWPE fibers have gained much attention due to their high strength and durability. Fiber reinforcement has been considered to improve the structural properties of the matrix when embedded within the polymer composite material [5]. In addition to fiber reinforcement, the addition of ceramic nanoparticles has also been considered to improve the mechanical and functional properties of the polymer composite material. Nano-hydroxyapatite (nHAp) has been considered to be an important addition to the polymer composite material due to its chemical composition, which is similar to that found in natural bone. Therefore, it may improve the biological response, which in turn may improve the mechanical properties of the polymer composite material [6]. Studies have shown that the addition of nHAp is a major contributor to improving the bioactivity and osteoconduction of polymers as well. For example, nHAp particles nucleate crystals, which make up the crystal lattice structure (increasing interface bonds between the UHMW-PE and the reinforcing fibers). In addition, the addition of low weight percentages of nHAp reportedly improves the hydrophilicity and surface energy of UHMWPE composites, which are important for the performance of implants in biomedicine [7]. Surface modification techniques are also commonly used to further improve the interactions between the polymer composite material and its environment. In this context, plasma treatment has been commonly reported to improve the surface properties of polymer composites without affecting their bulk properties [8]. It may improve the surface properties, which may further

improve the adhesion, friction, and biological response of the polymer composite material. Although UHMWPE fibers, nHAp particles, and plasma treatment have been used before in polymer composites, their combined use in a UHMWPE hybrid system still needs a clearer evaluation. In this type of material, the main challenge is to improve stiffness and wear resistance without losing too much tensile performance. The addition of nHAp can support bending and sliding behavior, but it may also affect the matrix–fiber interface if the particles are not distributed well. Plasma immersion ion implantation (PIII) treatment, on the other hand, is mainly a surface process, so its influence is expected to appear more in friction and wear than in the bulk mechanical response. For this reason, the present work studies UHMWPE composites reinforced with 40 wt.% UHMWPE fibers and different nHAp contents. After that, the selected hybrid composite was treated by PIII and examined by mechanical, thermal, morphological, dry-sliding wear, and in vitro cytocompatibility tests.

2. MATERIALS AND METHODS

2.1 Materials and composite preparation

Ultra-high molecular weight polyethylene UHMWPE powder was used as a matrix material in this research, with continuous fibers of UHMWPE used as a reinforcing material. The source of the UHMWPE powder used was Hangzhou Impact New Materials Co., Ltd., whereas continuous fibers were obtained from Beijing Tongyizhong New Material Technology Corporation. For nanoscale ceramic reinforcement, nHAp powder with an average diameter of 50 nm and a purity of 99% was used. The amount of fibers used in all reinforced composites was kept constant at 40 wt.%. The fiber properties were taken from the supplier information for the UHMWPE fibers used in this work. The reported fiber density was 0.97 g/cm³, with fineness of 1D–3.3D, model number 400D, tensile strength of 32–40 g/d, elastic modulus of 900–1400 g/d, and elongation at break of 2–3.5%. Using the reported fiber density, the 40 wt.% fiber content was estimated to be about 39.2 vol.%. The continuous fibers were manually placed in a unidirectional arrangement inside the mold. The number of layers and the spacing between fibers were adjusted by hand to reach the required fiber content. No extra chemical treatment was applied to the fibers before molding. During lay-up, the fibers were kept straight by manual alignment before hot pressing. Nano-hydroxyapatite in the reinforced composites was of 1, 2, and 3 wt.% relative to the total mass of the composite. In each composite composition and testing condition, three samples were prepared, and the reported value is the mean of the measurements (n = 3). The nano-hydroxyapatite powder was ultrasonically dispersed in ethanol for 30 minutes. After that, the dispersion of the nano-hydroxyapatite powder and the UHMWPE powder was mixed using a mechanical mixer for another 30 minutes to ensure the dispersion of the nano-hydroxyapatite powder. After this step, a drying process was conducted at a moderate temperature level until ethanol was completely evaporated. The dried powder mixture was then mixed using a ball milling machine for 2 hours in a ceramic milling jar with ceramic milling media of varying diameters. Composite samples were prepared using a thermo-compression molding machine. A steel mold of 160 × 100 × 4 mm was used to produce composite samples. The surface of the mold was cleaned with acetone before the implementation of each process, and then a release film was spread onto the inside surface of the mold for easier demolding. UHMWPE/nHAp powder mixture was filled into the mold cavity. Then, the UHMWPE continuous fiber was hand-laid in one direction inside the powder mixture. Then, the powder mixture was added to fill up the fibers, and then the mold was pressed under a hot press machine at 145 ℃ for 1 hr and 10MPa pressure. After this step, the mold was allowed to cool to ambient temperature before specimen extraction. An additional process of PIII was included for the hybrid composite with 40 wt. % fibers and 3 wt. % nano-hydroxyapatite. This process occurred under a pressure of 0.15 mbar, with a voltage of 800 V and a current of 15 mA for 10 hours under a nitrogen/hydrogen (N_2/H_2) plasma atmosphere. The process of plasma treatment was exclusively carried out on this hybrid composite material. Tribological tests were conducted on this material before and after the plasma treatment process.

2.2 Mechanical and tribological testing

Density measurement followed ASTM D792, in which Archimedes' principle is applied. Material hardness was measured using a Shore D hardness tester in accordance with ASTM D2240. Tensile testing followed ASTM D638, in which Type I specimens are required. Flexural testing followed ASTM D790, whereas impact resistance testing followed ISO 179. For the mechanical and tribological measurements, three specimens were tested for each composition or condition, and the reported values represent the average of these measurements. However, the individual replicate values were not available for all mechanical and tribological datasets; therefore, standard deviations, error bars, and statistical comparisons could not be reported for these results. Accordingly, these results are discussed only as observed average trends under the present experimental conditions. Tribological testing was done under dry sliding conditions according to ASTM G133. A 5 mm ceramic counter face was used under a normal load of 40 N. The sliding speed was 0.10 m/s, and the total sliding distance was 360 m. Throughout this process, the coefficient of friction was constantly monitored, and wear volume and wear coefficient were calculated. Wear tests were carried out for the composite containing 40 wt.% fibers, and for the hybrid composite containing 40 wt.% fibers and 3 wt.% nano-hydroxyapatite. The same hybrid composite was also tested after PIII. The present tribological tests were limited to dry sliding conditions. Therefore, the results are used to compare the relative wear behavior of the prepared composites under the selected test conditions. The schematic illustration of the proposed N_2/H_2 PIII mechanism is presented in Figure 1. During PIII treatment, the surface of the UHMWPE/nHAp hybrid composite is exposed to energetic plasma species. Based on previous reports on plasma-treated polymer surfaces, these species may interact with the outer polymer layer and may produce surface-related changes. Such changes may include bond scission, free-radical formation, limited surface cross-linking, or possible incorporation of nitrogen-containing groups. However, these mechanisms were not experimentally verified in the present study because surface-sensitive analyses such as X-ray photoelectron spectroscopy (XPS), contact-angle measurement, Atomic Force Microscopy (AFM), or nanoindentation were not performed. Therefore, the PIII-related explanation in this work is treated as a literature-

informed hypothesis, and the experimental conclusion is limited to the measured changes in friction and wear under dry-sliding conditions [9, 10].

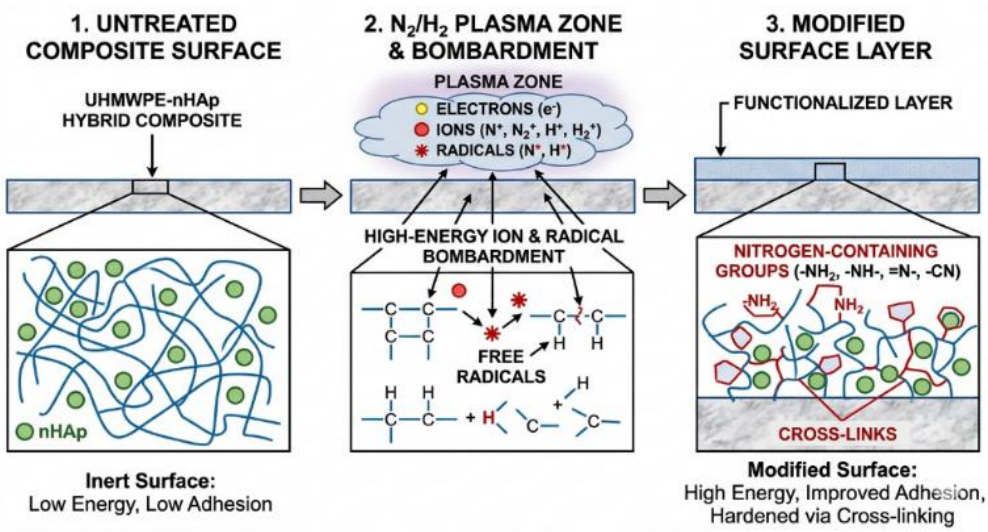

Figure 1. Schematic illustration of N_2/H_2 plasma immersion ion implantation (PIII) and its effect on the UHMWPE/nHAp hybrid composite surface (adapted from [9, 10])

Note: PIII = Plasma immersion ion implantation; UHMWPE = Ultra-high molecular weight polyethylene; nHAp = Nano-hydroxyapatite

2.3 Thermal and microstructural analysis

Thermal analysis was performed using differential scanning calorimetry (DSC). About 5 mg of each material was used for the analysis. Heating to 300 °C at a rate of 10 °C/min using sealed aluminum pans was conducted. Chemical characterization was conducted using Fourier-transform infrared spectroscopy (FTIR), whereas surface morphology analysis was conducted using field emission scanning electron microscopy (FESEM). The analysis was conducted on the composite material containing 40 wt.% fibers and the hybrid composite material containing 40 wt.% fibers and 3% wt. Nano-hydroxyapatite.

2.4 In vitro cytocompatibility 3-(4,5-dimethylthiazol-2-yl)-2,5-diphenyltetrazolium bromide assay

The cytocompatibility of the selected composite was evaluated by using the 3-(4,5-dimethylthiazol-2-yl)-2,5-diphenyltetrazolium bromide (MTT) assay. The sample used was the plasma-treated UHMWPE fiber/nHAp hybrid composite with 40 wt.% UHMWPE fibers and 3 wt.% nHAp. The composite samples were prepared in a solid square form with approximate dimensions of 2 × 2 cm. Since UHMWPE-based composites are chemically stable and insoluble in biological fluids, a direct contact test was used. Sterilized composite samples were placed directly into the cell culture wells. The tested cell lines were Human Dermal Fibroblast cells (HdFn) and Mg-63 bone-derived cells. Cell viability was recorded after 0, 24, 48, and 72 h of incubation. The MTT results were reported as mean ± standard deviation based on the available laboratory report. However, the available external laboratory report did not provide full details on the sterilization method, seeding density, culture medium composition, supplements, incubation atmosphere, control-group design, or the exact number and type of biological/technical replicates. Therefore, the MTT results are interpreted only as an initial in vitro cytocompatibility screening under the reported test conditions.

3. RESULTS AND DISCUSSION

3.1 Density

The density values for the prepared composites are presented in Figure 2. The density for the composite with 40 wt. % UHMWPE fibers was found to be 0.9496 g/cm³. When nano-hydroxyapatite particles are added to the composite, the density increases to 0.9518 g/cm³ for 1 wt. % nHAp, then to 0.9567 g/cm³ for 2 wt. %, and finally to 0.9755 g/cm³ for 3 wt. % particles. This shows an increasing trend, which follows the density difference between the two materials. The density of hydroxyapatite is greater than that of UHMWPE, and thus there is an increment in the mass of the composite by the addition of the particles in the matrix. An increase in density in a similar manner has been shown in hydroxyapatite-filled polymer composites [11]. The continuous increase in density is consistent with the addition of nHAp particles into the matrix material.

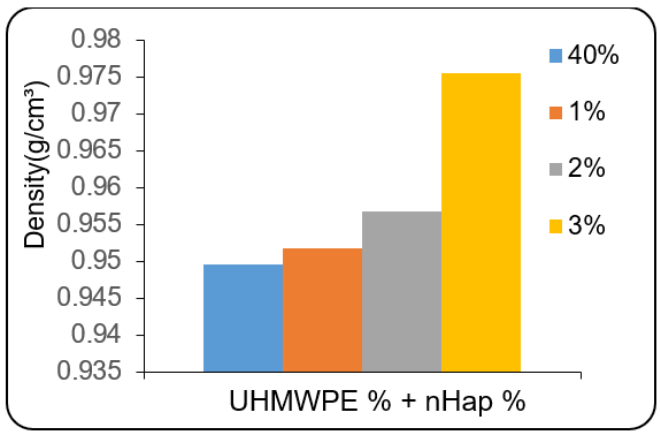

Figure 2. Variation in the density of UHMWPE composites reinforced with 40 wt.% fibers and different contents of nano-hydroxyapatite (0–3 wt.%)

3.2 Hardness

The values of Shore D hardness for the prepared composites are presented in Figure 3. The composite filled with 40 wt.% UHMWPE fibers had a hardness value of 62 Shore D. The values increased marginally with nano-hydroxyapatite content in composites filled with 1, 2, and 3 wt.% nHAp, with values of 62.3, 62.49, and 62.9, respectively. There is an increasing trend of hardness with increasing nHAp content. This small enhancement can perhaps be attributed to the existence of the hydroxyapatite within the UHMWPE. Usually, ceramics have more hardness in indentation compared to the polymer phase, as was observed in a work performed on polymer matrix composites filled with hydroxyapatite [12].

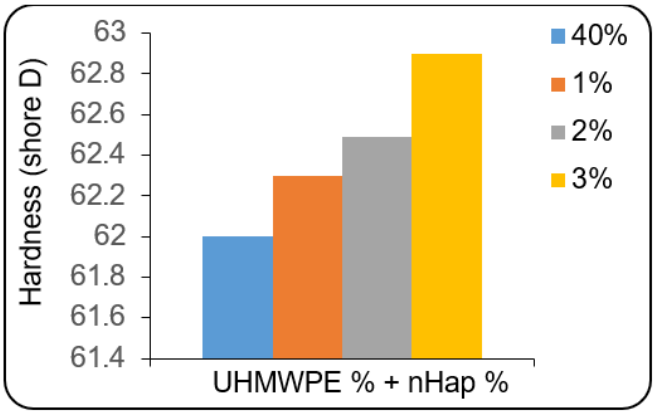

Figure 3. Shore D hardness values of UHMWPE composites containing 40 wt.% fibers with different nano-hydroxyapatite contents

3.3 Impact strength

Figure 4 shows the variation in impact strength. The impact strength of the 40 wt.% fiber-filled composite was found to be 0.0515 J/mm². After the introduction of nano-hydroxyapatite particles, the values increased to 0.0525 J/mm², 0.054 J/mm², and 0.055 J/mm² for 1, 2, and 3 wt.% nano-hydroxyapatite particles, respectively. The rise in value indicates that the nanoparticles affected the crack propagation behavior of the composite under rapid loading.

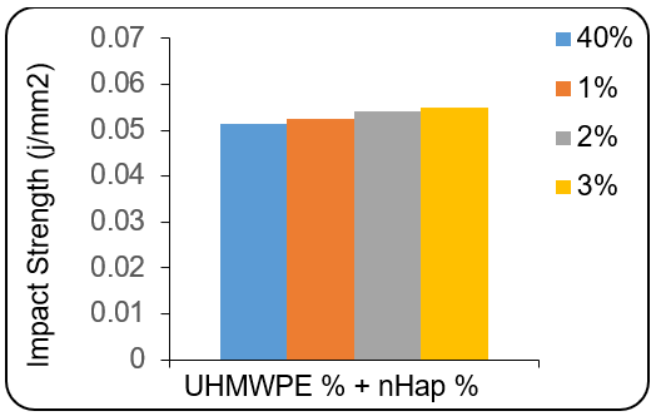

Figure 4. Impact strength of UHMWPE fiber composites as a function of nano-hydroxyapatite content

In polymeric materials, cracks usually propagate through the matrix phase. With the introduction of hydroxyapatite particles, the crack path may be disrupted, and crack growth may be retarded; therefore, higher energy is required to fracture the composite. Similar effects have been observed in hydroxyapatite-filled polymer composites [13].

3.4 Tensile properties

The tensile performance of the prepared composites can be analyzed from the stress-strain curves presented in Figure 5. An initial elastic deformation, which occurs in a linear regime, is seen, followed by non-linear plastic deformation of the composites [14]. The composite with 40 wt.% UHMWPE fibers exhibited the maximum tensile strength among the tested compositions. Moreover, the addition of nano-hydroxyapatite particles leads to slight changes in the morphology of the stress-strain curves. Thus, the composite with 1 wt. % nHAp has the lowest value of tensile strength but the highest value of strain at fracture, which may be evidence of improved ductility. When the amount of nHAp is increased to 2 wt. %, the value of strain at fracture is reduced. When the nHAp content increased to 3 wt.%, the tensile strength increased compared with the 1 wt.% and 2 wt.% nHAp samples, but it was still slightly lower than the fiber-only composite. This means that the addition of nHAp did not improve the tensile strength in a direct way. The reduction may be related to particle agglomeration, local weak regions, or changes at the matrix–fiber interface [15].

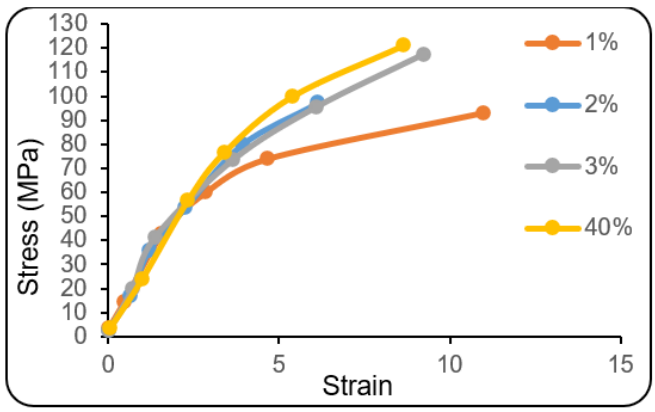

Figure 5. Stress–strain curves of UHMWPE composites reinforced with 40 wt.% fibers and different nano-hydroxyapatite contents

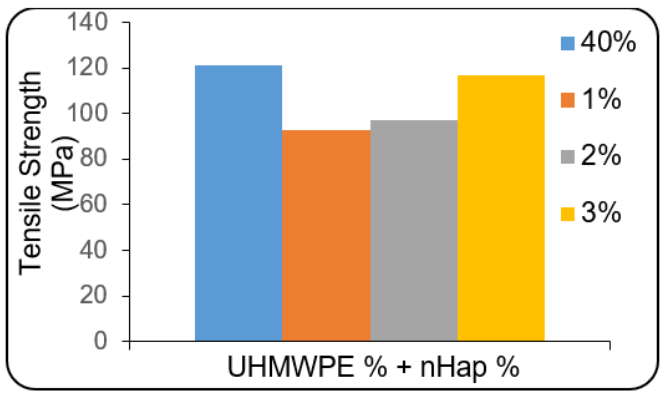

Figure 6. Tensile strength of UHMWPE composites reinforced with 40 wt.% fibers and varying nano-hydroxyapatite content

Figure 6 depicts the tensile strength of the composites. A composite of 40 wt.% fibers and no nanoparticles have a tensile strength of 121 MPa, which was reduced to 93 MPa by the addition of 1 wt % nHAp. When 2 wt % nHAp was added, the tensile strength of the composite was 97 MPa. When the nanoparticle content reached 3 wt.%, the tensile strength increased again to 117 MPa. The reduction in tensile strength after adding 1 wt.% and 2 wt.% nHAp may be associated with local stress concentration, particle agglomeration, or weaker regions at the matrix–fiber interface. At 3 wt.% nHAp, the tensile strength increased again compared with the lower nHAp contents, but it did not exceed the value of the fiber-reinforced composite without nHAp. Therefore, the tensile results suggest that nHAp addition improved the stiffness more clearly than the tensile strength [16].

The elastic modulus increased slightly from 2.36 GPa to 2.44 GPa, indicating that the composite became somewhat stiffer after adding hydroxyapatite particles, as shown in Figure 7 [17]. The elongation at failure ranged from 6% to 10.5%, as illustrated in Figure 8, suggesting a change in deformation behavior with increasing nanoparticle content [18].

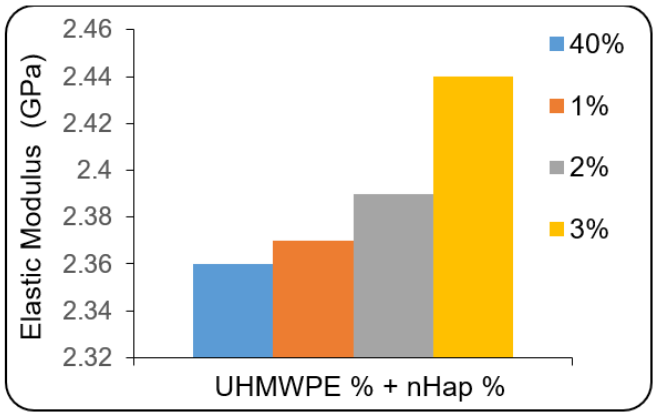

Figure 7. Elastic modulus of UHMWPE composites containing 40 wt.% fibers with different nano-hydroxyapatite additions

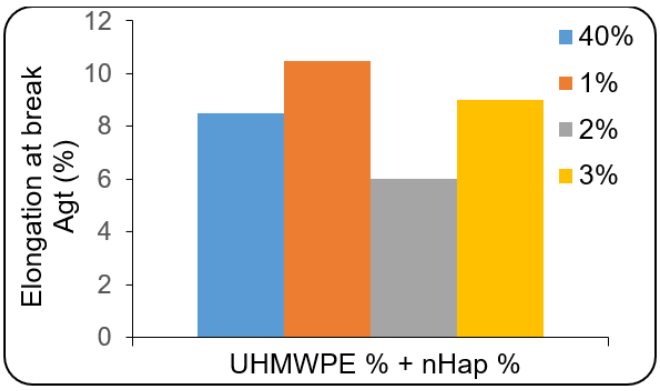

Figure 8. Elongation at break of UHMWPE composites reinforced with fibers and nano-hydroxyapatite

3.5 Flexural properties

Figure 9 shows the flexural properties of the composites using the three-point bending test. A composite containing 40 wt.% fibre showed a flexural strength of 21.6 MPa, and the value increased to 25.8 MPa for 1 wt.% nano-hydroxyapatite, 37.2 MPa for 2 wt.% nano-hydroxyapatite, and 39 MPa for 3 wt.% nano-hydroxyapatite. During the flexural testing of the specimen, the composite is placed under tension on one side and compression on the other side. Under these circumstances, the composite becomes more rigid as it incorporates more nanoparticles [19].

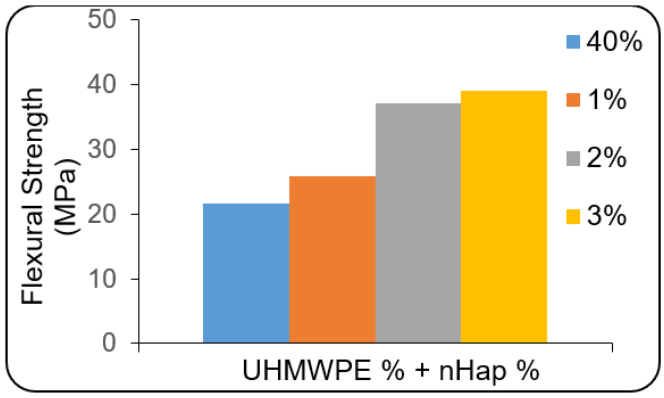

Figure 9. Flexural strength of UHMWPE fiber composites with different nano-hydroxyapatite contents obtained from the three-point bending test

The flexural modulus increased from 0.592 GPa to 1.954 GPa with the incorporation of nanoparticles, as shown in Figure 10, indicating a marked increase in the stiffness of the composite structure [20].

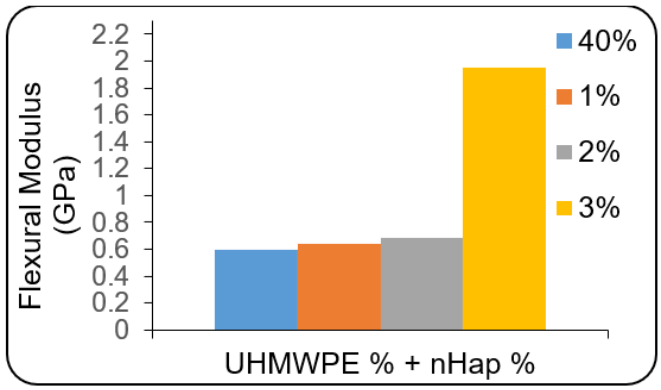

Figure 10. Flexural modulus of UHMWPE composites reinforced with 40 wt.% fibers and nano-hydroxyapatite

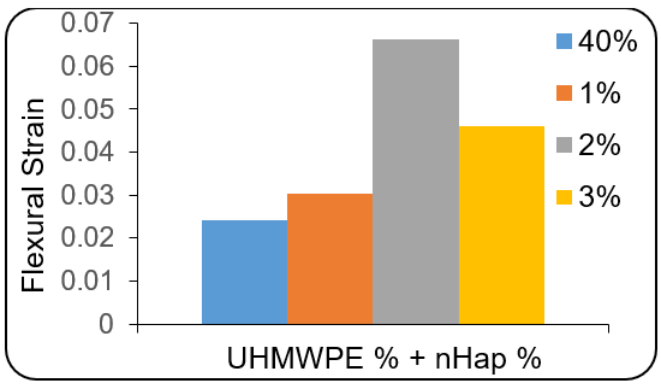

Figure 11. Flexural strain behavior of UHMWPE composites under bending load

The flexural strain behavior of the composite is shown in

Figure 11, where the deformation behavior of the composite is clearly illustrated. Figure 12 shows the maximum shear stress values obtained during the flexural test. The maximum shear stress values increase, starting from 0.675 MPa for the composite reinforced by fibers to 1.219 MPa for the composite reinforced by 3 wt.% nano-hydroxyapatite, as shown in Figure 12. This is an indication that the addition of nanoparticles enhances the shear deformation resistance of the composite under bending. The addition of hydroxyapatite particles helps in the distribution of the stress in the matrix, delaying shear deformation [21].

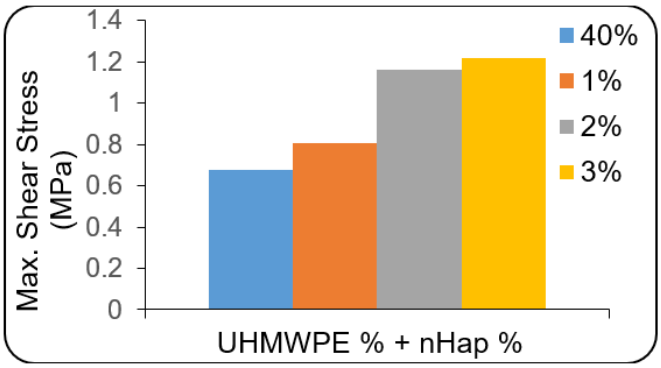

Figure 12. Maximum shear stress (τmax) obtained during flexural testing for UHMWPE composites with different nano-hydroxyapatite contents

3.6 Selection of the composite for further characterization

Based on the average results obtained in the present study, the composite containing 40 wt.% UHMWPE fibers and 3 wt.% nHAp was selected for further characterization. This selection was limited to the composition range tested in this work and should not be interpreted as a universal optimum formulation. The selection was based on a combined comparison of the measured responses, including flexural strength, flexural modulus, maximum shear stress, dry-sliding wear response, and tensile strength retention relative to the fiber-reinforced composite without nHAp. Therefore, the 3 wt.% nHAp composite was used as the selected formulation for the additional FTIR, DSC, FESEM, wear, PIII treatment, and cytocompatibility evaluations. FTIR, DSC, and FESEM analyses were performed for two compositions: (i) the composite containing 40 wt.% UHMWPE fibers and (ii) the hybrid composite containing 40 wt.% UHMWPE fibers and 3 wt.% nHAp. Wear behavior has been assessed for the 40 wt% fiber composite and 40 wt% fiber/3 wt% nHAp hybrid composite, and the treated hybrid composite after PIII surface treatment.

3.7 Fourier-transform infrared spectroscopy analysis

Figure 13 shows the FTIR spectra of the composites: (a) UHMWPE composite reinforced with 40 wt.% fibers, and (b) hybrid composite reinforced with 40 wt.% fibers and 3 wt.% nano-hydroxyapatite. The composite is primarily composed of UHMWPE and hence shows bands corresponding to polyethylene. Two bands corresponding to asymmetric and symmetric stretching of CH_2 groups in the polymer chain of polyethylene appear at 2924 cm^{-1} and 2851 cm^{-1}. Besides that, bands at 1465 cm^{-1} and 720 cm^{-1} may be attributed to the bending and rocking of CH_2 groups in the polymer chain of UHMWPE, as is commonly observed in materials containing UHMWPE [22]. After incorporating 3 wt.% nano-hydroxyapatite, additional peaks appear in the FTIR spectrum of the hybrid composite. A prominent peak at about 1080 cm^{-1} indicates the stretching vibration of phosphate groups, which are characteristic of hydroxyapatite. In addition, a peak observed near 632 cm^{-1} is associated with the OH vibration mode of hydroxyapatite [23]. The presence of these bands indicates the incorporation of hydroxyapatite particles in the polymer matrix. From a comparison of the two spectra, it is clear that all the characteristic bands of UHMWPE are present in the hybrid composite material, and in addition, there are bands corresponding to phosphate groups, indicating the presence of nano-hydroxyapatite in the composite material.

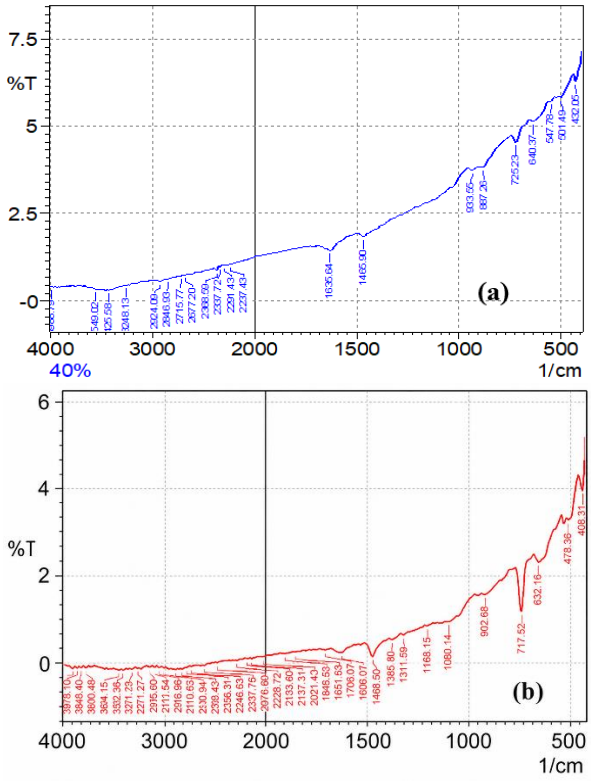

Figure 13. FTIR spectra of (a) UHMWPE composite reinforced with 40 wt.% fibers and (b) hybrid composite reinforced with 40 wt.% fibers and 3 wt.% nano-hydroxyapatite
Note: FTIR = Fourier-transform infrared spectroscopy

3.8 Differential scanning calorimetry analysis

DSC analysis of the composites studied is shown in Figure 14. The composite, which has 40% by weight of UHMWPE fibers, shows a melting point of about 136 °C; the melting begins at roughly 129 °C and finishes close to 140 °C. This point matches the melting of the crystalline part of the UHMWPE. The melting temperature found in this work is within what is normally found for UHMWPE – it usually melts from 130 °C to 138 °C, because of its semi-crystalline nature and the length of its polymer chains [24]. The hybrid composite with 3 % by weight of nano-hydroxyapatite, however, shows a melting point of about 138.8 °C, a little higher than that of the fiber-reinforced composite. This change means that nano-hydroxyapatite affects how the UHMWPE matrix crystallizes. In polymer nanocomposites, ceramic nanoparticles can work as different places for crystallization

to start, which may promote the formation of more stable crystalline regions in the polymer's build [25]. A small rise in melting temperature can be the outcome. Besides the main melting change, the hybrid composite's thermal diagram also shows other thermal events at higher temperatures, at around 256 ℃ and 271 ℃. These thermal signs are linked to other thermal processes in the composite system, and could be due to changes in structure or links between the polymer, which forms the main body, and the ceramic, which is spread through it [26]. Even with these differences, the DSC results show that adding nano-hydroxyapatite does not change the main thermal behavior of UHMWPE in a big way, but does change the melting a little, because of links between polymer and particle.

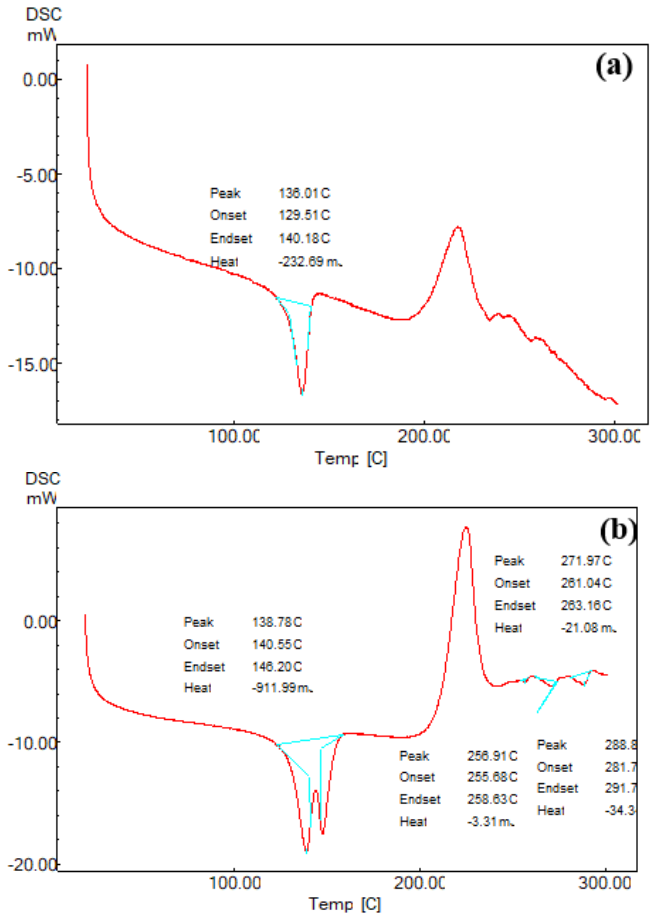

Figure 14. DSC thermograms of (a) UHMWPE composite reinforced with 40 wt.% fibers and (b) hybrid composite containing 40 wt.% fibers with 3 wt.% nano-hydroxyapatite
Note: DSC = Differential scanning calorimetry

3.9 Field emission scanning electron microscopy morphology

Scanning electron microscopy with field emission (FESEM) has been used to study the microstructure of the composites. The micrographs obtained are presented in Figure 15, which were obtained using 20 µm and 100 µm scale bars. The study compares the fracture response of 40 wt.% UHMWPE fiber-reinforced composites with 40 wt.% fiber-3 wt.% nano-hydroxyapatite hybrid composites. In the 40 wt.% fiber composites, the FE-SEM micrograph shows the microstructure, which can be considered similar to that of fiber-reinforced composites made with polymers. In this figure, it can be noted that UHMWPE fibers are well embedded in the matrix; however, there are certain regions where the fibers are only partially embedded, with a gap between the fiber surface and the matrix surface. It can be noted that there is fiber-matrix debonding during fracture. In addition, the surface of the fibers has an irregular shape with small voids present in the matrix, which can be attributed to the debonding between the fiber surface and the matrix surface [27].

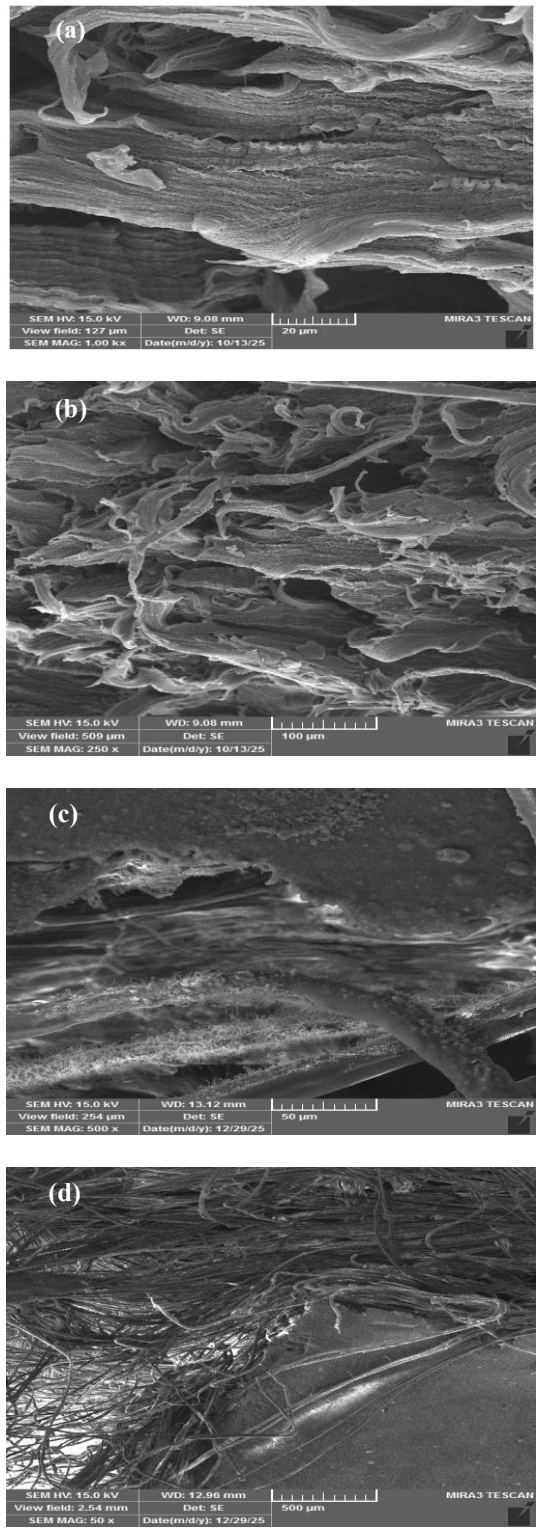

Figure 15. FESEM micrographs of UHMWPE composites: (a) 40 wt.% fiber composite at 20 µm, (b) 40 wt.% fiber composite at 100 µm, (c) hybrid composite (40 wt.% fibers + 3 wt.% nHAp) at 50 µm, (d) hybrid composite (40 wt.% fibers + 3 wt.% nHAp) at 500 µm
Note: FESEM = Field emission scanning electron microscopy

On the other hand, a densely packed microstructure is observed in the hybrid composite reinforced with 3 wt.% nano-hydroxyapatite. The polymer matrix appears to be in closer contact with the fiber surfaces. There are fewer discontinuities at the interface between the matrix material and the fibers compared to the discontinuities between the fibers only. In addition, with increased magnification, it can be seen that there are bright spots in the matrix material. These bright regions may be related to the presence of nano-hydroxyapatite within the UHMWPE phase. These observations are consistent with the presence of ceramic particles within the polymer matrix. The hybrid composite also contains regions where bridging of adjacent fibers takes place through a polymer matrix. This morphology might be responsible for the stress transfer from the matrix to the fibers, which also explains that flexural property increases. The results correlate well with the mechanical tests, especially with flexural properties and maximum shear stress of the hybrid composite. Similar observations have been reported for UHMWPE composites containing nano-hydroxyapatite, where ceramic particles were associated with changes in the internal morphology of the composite [28].

3.10 Wear behavior

The tribological behavior of the studied composites was evaluated under dry sliding conditions, and the corresponding results are presented in Figures 16–21. These results are discussed as average trends under the selected dry-sliding condition, because individual replicate values were not available for calculating standard deviations or error bars. The tribological characteristics are based on the wear response of the composite with 40 wt.% UHMWPE fibers, the composite with 40 wt.% UHMWPE fibers and 3 wt.% nano-hydroxyapatite, and the same hybrid composite after plasma treatment. The comparison allows a limited assessment of the influence of nHAp addition and PIII surface treatment on the measured friction and wear responses under the present test condition.

3.10.1 Coefficient of friction

The variation of the coefficient of friction (COF) with the sliding distance for the investigated composites is shown in Figures 16 and 17. The friction curves of the composites show an initial running-in phase, followed by a relatively stable phase of sliding. The friction behavior of the investigated composites is typical of polymer-based tribological systems, in which the surfaces in contact tend to gradually conform during the initial phase of the test [29]. Figure 16 compares the friction behavior of the composite reinforced with 40 wt.% fibers with that of the hybrid composite containing 3 wt.% nano-hydroxyapatite. The friction coefficient of the composite reinforced with fibers is higher, with an average value of 0.20, whereas the friction coefficient of the hybrid composite is relatively lower, with an average value of 0.144. The lower average friction coefficient of the hybrid composite may be related to the presence of nano-hydroxyapatite particles in the UHMWPE matrix. These particles may contribute to load sharing during dry sliding and may reduce direct polymer deformation at the contact surface. However, this explanation remains a possible interpretation because wear-track analysis, transfer-film observation, and counterface examination were not performed in the present study. Therefore, the comparison is limited to the measured average COF values under the selected dry-sliding condition [30]. The effect of plasma treatment on the friction behavior of the hybrid composite material is shown in Figure 17. The average friction coefficient changed from 0.144 before plasma treatment to 0.138 after plasma treatment. Because this change is small and no surface-sensitive analysis was performed, it is discussed only as a possible surface-related response under the present dry-sliding condition. Since PIII is a surface treatment, this response may be related to changes in the outer surface of the hybrid composite, this explanation remains unverified in the present work [31].

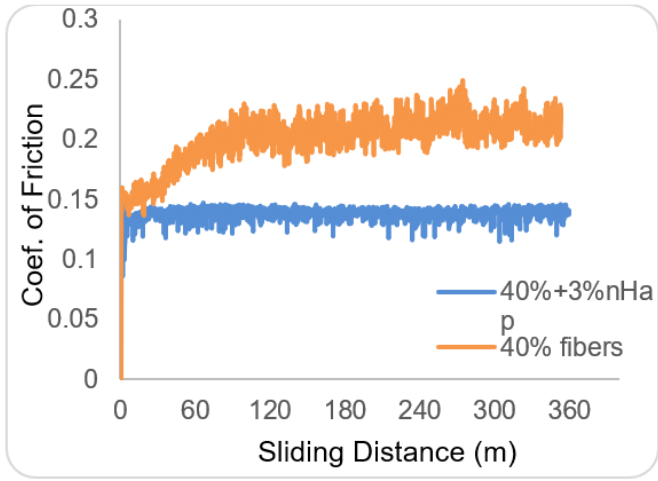

Figure 16. Coefficient of friction versus sliding distance for 40 wt.% UHMWPE fiber composite and hybrid composite containing 3 wt.% nano-hydroxyapatite

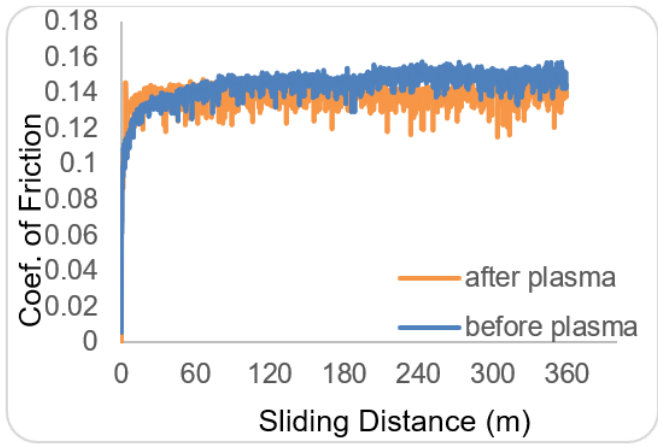

Figure 17. Coefficient of friction versus sliding distance for the hybrid composite before and after plasma treatment

3.10.2 Wear coefficient

The wear coefficient values of the investigated composites are presented in Figures 18 and 19. The addition of 3 wt.% nano-hydroxyapatite was associated with a lower average wear coefficient under the present dry-sliding condition. As shown in Figure 18, the average wear coefficient decreased from 4.45×10^{-4} for the 40 wt.% fiber composite to 2.20×10^{-4} for the hybrid composite containing 3 wt.% nHAp. This lower average value may be related to the presence of ceramic particles in the UHMWPE matrix, which may contribute to load sharing and reduce surface deformation during sliding. However, this explanation is treated as a possible mechanism because wear-track morphology and counterface analysis were

not performed [32]. Figure 19 shows the wear coefficient of the hybrid composite before and after PIII treatment. The average value changed slightly from 2.20 × 10^{-4} before treatment to 2.17 × 10^{-4} after treatment. Because this change is small and no surface-chemistry analysis was performed, it is discussed only as a possible surface-related response under the present dry-sliding condition. Plasma treatment may affect polymer surface characteristics according to previous reports, but this mechanism was not directly confirmed in the present work [33].

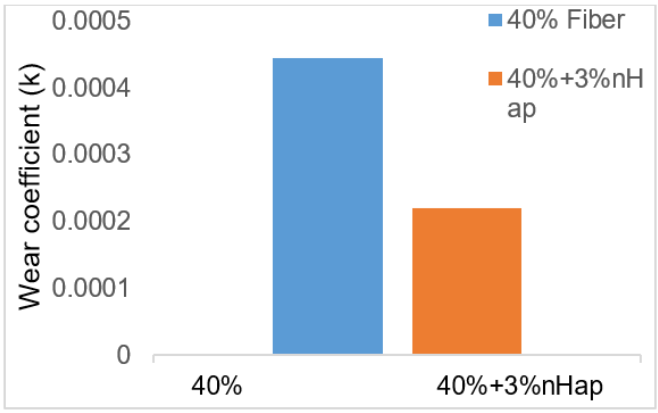

Figure 18. Comparison of wear coefficient for the composite reinforced with 40 wt.% fibers and the hybrid composite containing 3 wt.% nano-hydroxyapatite

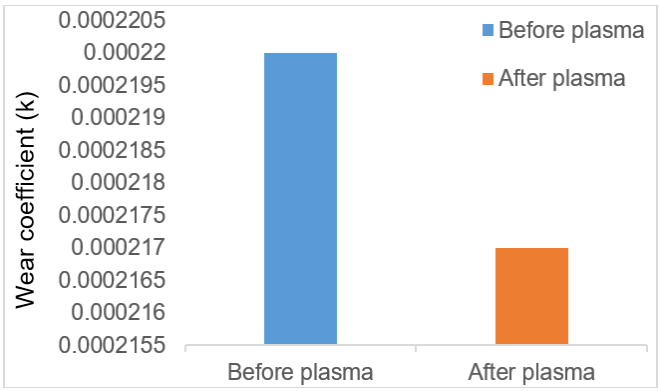

Figure 19. Comparison of wear coefficient for the hybrid composite before and after plasma treatment

3.10.3 Wear volume

The wear volume results obtained from the sliding tests are presented in Figures 20 and 21. The hybrid composite containing 3 wt.% nHAp showed a lower average wear volume than the 40 wt.% fiber composite under the present dry-sliding condition. As shown in Figure 20, the average wear volume changed from 0.048986 mm³ for the 40 wt.% fiber composite to 0.024177 mm³ for the hybrid composite. This lower average value may be associated with the presence of nano-hydroxyapatite particles in the matrix; however, the exact wear mechanism was not directly confirmed because wear-track SEM, transfer-film observation, and counterface analysis were not performed. Figure 21 presents the comparison between the hybrid composite before and after PIII treatment. The average wear volume changed slightly from 0.024177 mm³ before plasma treatment to 0.023905 mm³ after plasma treatment. Since PIII is a surface treatment, this small change may be related to changes occurring at the outer polymer surface rather than to bulk modification of the composite. Previous studies have reported that plasma treatment can alter polymer surface characteristics, including surface chemistry and surface activity [34]. In addition, limited surface cross-linking or surface chemical changes have been reported for plasma-treated polymer surfaces [35]. However, these surface changes were not directly confirmed in the present work because surface-sensitive analyses were not performed. Therefore, the wear-volume change after PIII treatment is discussed only as a possible surface-related response under the present dry-sliding condition.

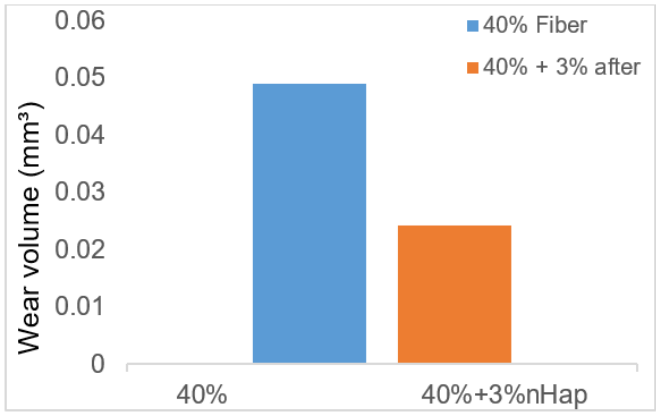

Figure 20. Comparison of wear volume for the composite containing 40 wt.% fibers and the hybrid composite containing 3 wt.% nano-hydroxyapatite

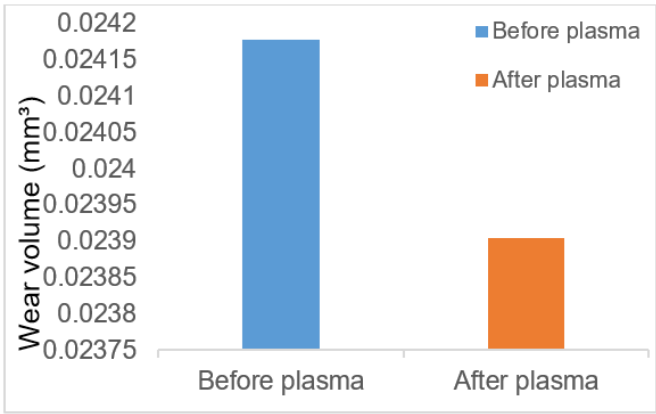

Figure 21. Comparison of wear volume for the hybrid composite before and after plasma surface treatment

3.11 In vitro cytocompatibility

Figure 22 shows the cell viability evaluated by the MTT assay for both HdFn and Mg-63 cell lines after 0, 24, 48, and 72 h of incubation with the selected composite. Cell viability values were above 90% during the whole test period for both cell lines. HdFn viability decreased from 99.053 ± 0.550% at 0 h to 95.782 ± 0.648% at 72 h, while Mg-63 cell viability decreased from 98.264 ± 0.834% at 0 h to 94.715 ± 0.067% at 72 h. Although a decrease was observed with increasing incubation time, the results remained within an acceptable range under the present in vitro conditions [36].

A direct comparison between the two cell lines is presented in Figure 23. The MTT results showed that cell viability remained above 90% for both HdFn and Mg-63 cells under the reported test conditions. However, because some procedural

details were not available from the external laboratory report, including the exact control-group design and replicate structure, these results should be interpreted only as an initial in vitro cytocompatibility screening. Further biological testing with fully reported experimental conditions is required before making broader conclusions about biomedical applicability [37].

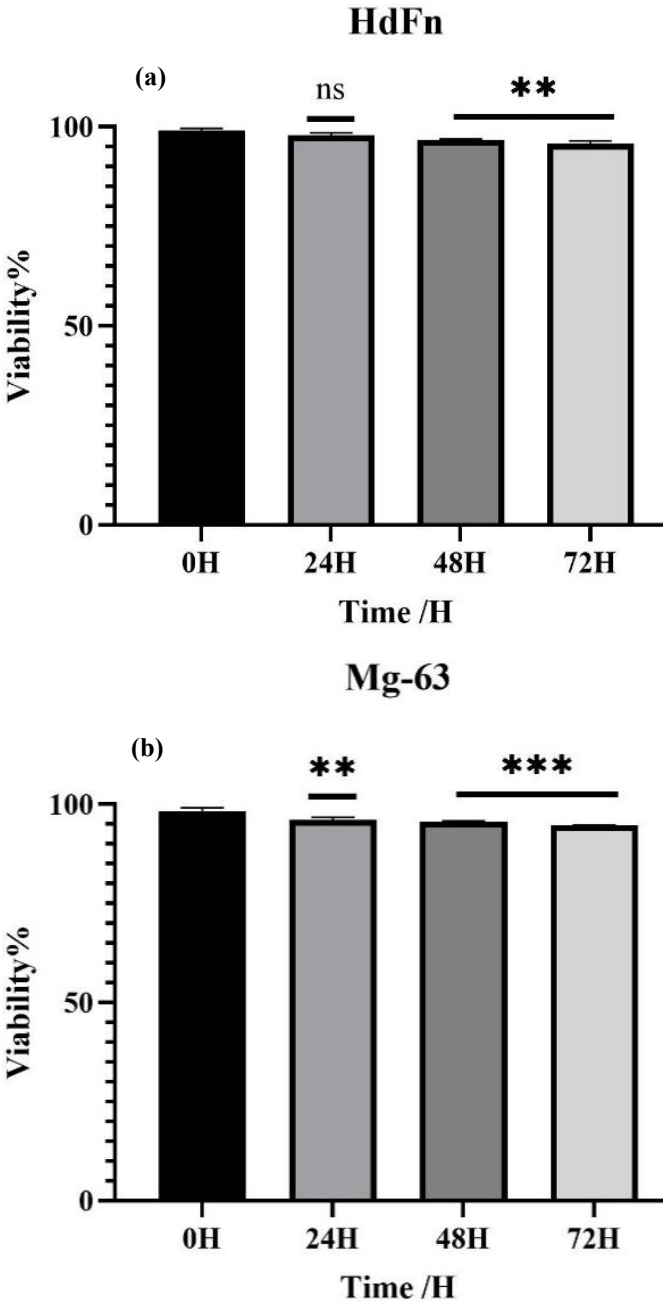

Figure 22. Cell viability determined by the MTT assay for the selected composite at different incubation times (0, 24, 48, and 72 h): (a) HdFn cell line and (b) Mg-63 cell line
Note: HdFn = Human dermal fibroblast cells
Note: MTT = 3-(4,5-dimethylthiazol-2-yl)-2,5-diphenyltetrazolium bromide

Before exposure, the control cells were spread on the surface and showed a spindle-like form with good attachment. After contact with the UHMWPE fiber/nHAp hybrid composite, the cells kept a close general appearance to the control cells, and no clear cell detachment or obvious morphological damage was seen, as shown in Figure 24. The cell images also agree with the MTT data, where the measured viability stayed above 90% during the test period [36]. These images are therefore used only as supporting observations and not as a full biological evaluation of the material.

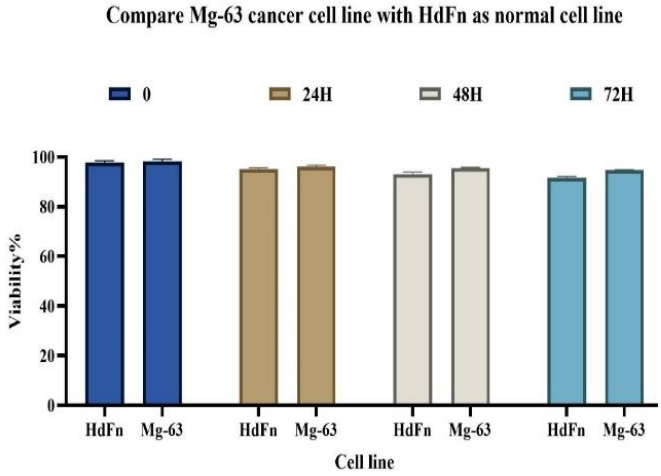

Figure 23. Comparison of cell viability between HdFn and Mg-63 cell lines after exposure to the selected composite at different incubation periods

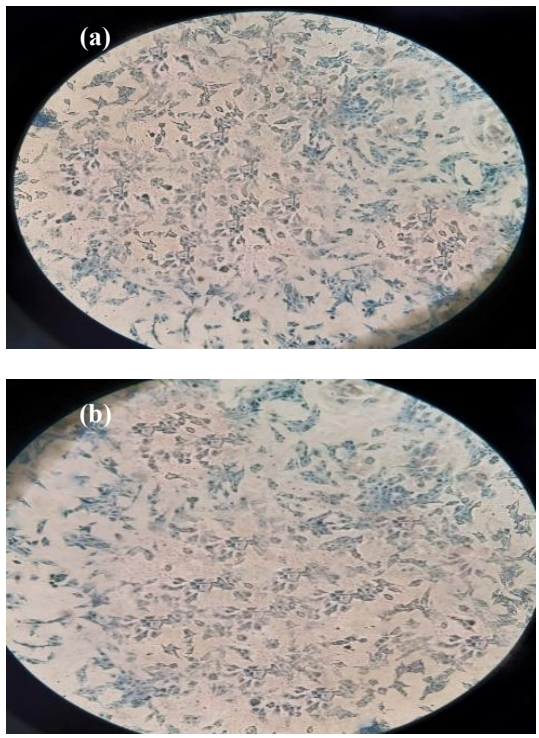

Figure 24. Microscopic images of HdFn cells used for the MTT assay: (a) control cells before exposure, (b) cells after exposure to the UHMWPE fiber/nHAp composite
Note: MTT = 3-(4,5-dimethylthiazol-2-yl)-2,5-diphenyltetrazolium bromide

4. LIMITATIONS AND FUTURE WORK

The present work was performed under controlled laboratory conditions, so the results should be interpreted within these conditions. The wear tests were carried out under dry sliding, while real biomedical contacts usually work in lubricated environments. For this reason, future studies should include wear tests in simulated body fluid, Phosphate-Buffered Saline (PBS), or other lubricated media. Another

limitation is that the individual replicate values were not available for all mechanical and tribological datasets. Therefore, standard deviations, error bars, and statistical tests could not be added for these results. The comparisons are consequently limited to the observed average trends, and stronger statistical conclusions require future testing with fully reported replicate data. Also, PIII treatment was applied only to the selected composite containing 40 wt.% fibers and 3 wt.% nHAp. More treatment groups are needed in future work to separate the effect of nHAp from the effect of plasma treatment. In addition, direct porosity measurement and more detailed fiber distribution analysis should be included to support the interpretation of the composite structure. The explanation of the plasma-treated surface should also be supported in future work by surface tests such as XPS, contact angle, AFM, or nanoindentation. The biological part was limited to the MTT assay on HdFn and Mg-63 cells, and the available external laboratory report did not provide all procedural details such as seeding density, culture medium composition, sterilization method, incubation atmosphere, control-group design, or the exact replicate structure. Therefore, the biological results should be interpreted only as an initial in vitro screening under the reported conditions, and longer cell studies and in vivo tests are still required before making broader conclusions about biomedical use.

5. CONCLUSION

The composites in this study were prepared using 40 wt.% UHMWPE fibers with different additions of nHAp. After comparing the tested samples, the material containing 3 wt.% nHAp was taken forward to the PIII treatment step. The average density, hardness, and impact strength values became higher as nHAp was added to the UHMWPE matrix. This 3 wt.% nHAp sample was also chosen for the later characterization work because it gave higher average bending-related values, including flexural strength, flexural modulus, and maximum shear stress. At the same time, its tensile strength stayed close to that of the fiber composite without nHAp. The FTIR spectra showed the main UHMWPE bands together with phosphate-related bands from nHAp. DSC analysis showed only a small change in the melting behavior after nHAp addition, so the main thermal behavior of UHMWPE was mostly retained. The FESEM images showed a more compact-looking morphology in the hybrid composite; however, the interface quality and particle distribution were not measured quantitatively. Under dry sliding conditions, the hybrid composite gave lower average friction and wear-volume values than the fiber composite without nHAp. After PIII treatment, the selected hybrid composite showed a further small decrease in the average friction and wear values. This change is discussed only as a possible surface-related response under the dry-sliding condition used in this study, because surface-sensitive tests were not carried out. The MTT assay showed cell viability above 90% for both HdFn and Mg-63 cell lines under the reported test conditions. Still, the biological test was limited to an initial in vitro screening, and some procedural details were not available from the external laboratory report. For this reason, further biological testing with fully reported experimental conditions is needed before making broader conclusions about biomedical applicability.

AI STATEMENT

Generative AI tools were used solely for language refinement and structural improvement.

REFERENCES

[1] Hussain, M., Naqvi, R.A., Abbas, N., Khan, S.M., Nawaz, S., Hussain, A., Zahra, N., Khalid, M.W. (2020). Ultra-high-molecular-weight-polyethylene (UHMWPE) as a promising polymer material for biomedical applications: A concise review. Polymers, 12(2): 323. https://doi.org/10.3390/polym12020323

[2] Hasegawa, M., Tone, S., Naito, Y., Sudo, A. (2023). Ultra-high-molecular-weight polyethylene in hip and knee arthroplasties. Materials, 16(6): 2140. https://doi.org/10.3390/ma16062140

[3] Wahed, S.B., Dunstan, C.R., Boughton, P.C., Ruys, A.J., Faisal, S.N., Wahed, T.B., Salahuddin, B., Cheng, X., Zhou, Y., Wang, C.H., Islam, M.S., Aziz, S. (2022). Functional ultra-high molecular weight polyethylene composites for ligament reconstructions and their targeted applications in the restoration of the anterior cruciate ligament. Polymers, 14(11): 2189. https://doi.org/10.3390/polym14112189

[4] Du, M.Z., Chen, J.D., Liu, K.H., Xing, H.R., Song, C. (2021). Recent advances in biomedical engineering of nano-hydroxyapatite including dentistry, cancer treatment and bone repair. Composites Part B: Engineering, 215: 108790. https://doi.org/10.1016/j.compositesb.2021.108790

[5] Fiume, E., Magnaterra, G., Rahdar, A., Verné, E., Baino, F. (2021). Hydroxyapatite for biomedical applications: A short overview. Ceramics, 4(4): 542-563. https://doi.org/10.3390/ceramics4040039

[6] Mondal, S., Park, S., Choi, J., Vu, T.T.H., Doan, V.H.M., Vo, T.T., Lee, B., Oh, J. (2023). Hydroxyapatite: A journey from biomaterials to advanced functional materials. Advances in Colloid and Interface Science, 321: 103013. https://doi.org/10.1016/j.cis.2023.103013

[7] Senra, M.R., Marques, M.F.V., Souza, D.H.S. (2020). Ultra-high molecular weight polyethylene bioactive composites with carbonated hydroxyapatite. Journal of the Mechanical Behavior of Biomedical Materials, 110: 103938. https://doi.org/10.1016/j.jmbbm.2020.103938

[8] He, J., Wang, Y., Qian, Y., Guo, J.S., Lu, J.X., Yang, W.C. (2024). Surface modification of ultra-high-molecular-weight polyethylene and applications: A review. Polymers, 16(23): 3431. https://doi.org/10.3390/polym16233431

[9] Turicek, J., Ratts, N., Kaltchev, M., Masoud, N. (2021). Surface treatment of ultra-high molecular weight polyethylene (UHMWPE) by cold atmospheric plasma (CAP) for biocompatibility enhancement. Applied Sciences, 11(4): 1703. https://doi.org/10.3390/app11041703

[10] Kondyurin, A., Naseri, P., Fisher, K., McKenzie, D.R., Bilek, M.M.M. (2009). Mechanisms for surface energy changes observed in plasma immersion ion implanted polyethylene: The roles of free radicals and oxygen-containing groups. Polymer Degradation and Stability, 94(4): 638-646. https://doi.org/10.1016/j.polymdegradstab.2009.01.004

[11] Aiza Jaafar, C.N., Zainol, I., Izyan Khairani, M.I., Dele-Afolabi, T.T. (2022). Physical and mechanical properties of tilapia scale hydroxyapatite-filled high-density polyethylene composites. Polymers, 14(2): 251. https://doi.org/10.3390/polym14020251

[12] Kadhim, T.R., Oleiwi, J.K., Hamad, Q.A. (2023). Improving the biological properties of UHMWPE biocomposite for orthopedic applications. International Journal of Biomaterials, 2023: 4219841. https://doi.org/10.1155/2023/4219841

[13] Verma, N., Keshri, A.K., Pathak, H., Zafar, S., Prasad, A. (2022). Mesoscale modeling and biocompatibility of nano-hydroxyapatite reinforced ultra-high molecular weight polyethylene composite. Proceedings of the Institution of Mechanical Engineers, Part C: Journal of Mechanical Engineering Science, 236(8): 4267-4285. https://doi.org/10.1177/09544062211050456

[14] Arulraj, V., Datta, S., Davim, J.P. (2022). Natural computing-based designing of hybrid UHMWPE composites for orthopedic implants. Applied Sciences, 12(20): 10408. https://doi.org/10.3390/app122010408

[15] Efe, G., Altınsoy, İ., Türk, S., Bindal, C. (2020). An investigation on UHMWPE-HAp composites manufactured by solution-gelation method. Sakarya University Journal of Science, 24(1): 1-9. https://doi.org/10.16984/saufenbilder.396984

[16] Verma, N., Pathak, H., Keshri, A.K., Prasad, A., Zafar, S. (2022). Influence of UV exposure on mechanical behavior and cellular compatibility of nano-hydroxyapatite reinforced ultra-high molecular weight polyethylene. Materials Today Communications, 31: 103542. https://doi.org/10.1016/j.mtcomm.2022.103542

[17] Vinoth, A., Dey, S., Datta, S. (2021). Designing UHMWPE hybrid composites using machine learning and metaheuristic algorithms. Composite Structures, 267: 113898. https://doi.org/10.1016/j.compstruct.2021.113898

[18] Nayak, C., Ariharan, S., Kundu, B., Singh, S., Sivakumar, S., Balla, V.K., Balani, K. (2021). Radiation-induced effects on micro-scratch of ultra high molecular weight polyethylene biocomposites. Journal of Materials Research and Technology, 12: 2277-2293. https://doi.org/10.1016/j.jmrt.2021.02.040

[19] Singh, R.K., Gangwar, S., Singh, D.K. (2023). Experimental analysis with GRA-PCA-based hybrid optimization to analyze the effect of hydroxyapatite nanoparticle-reinforced UHMWPE for hip joint. Journal of Advanced Manufacturing Systems, 22(2): 423-444. https://doi.org/10.1142/S021968672350021X

[20] Çelebi Efe, G.F., Yener, T., Zor, M.S., Türk, S., Bindal, C. (2025). Characterization of enhanced UHMWPE-HAp composites manufactured by hot pressing. Polymer Composites, 16: 15102-15114. https://doi.org/10.1002/pc.30116

[21] Nabhan, A., Sherif, G., Abouzeid, R., Taha, M. (2023). Mechanical and tribological performance of HDPE matrix reinforced by hybrid Gr/TiO2 NPs for hip joint replacement. Journal of Functional Biomaterials, 14(3): 140. https://doi.org/10.3390/jfb14030140

[22] Han, L., Cai, H.F., Chen, X., Zheng, C., Guo, W.H. (2020). Study of UHMWPE fiber surface modification and the properties of UHMWPE/epoxy composite. Polymers, 12(3): 521. https://doi.org/10.3390/polym12030521

[23] Hossain, M.S., Ahmed, S. (2023). FTIR spectrum analysis to predict the crystalline and amorphous phases of hydroxyapatite: A comparison of vibrational motion to reflection. RSC Advances, 13(21): 14625-14630. https://doi.org/10.1039/D3RA02580B

[24] Dayyoub, T., Olifirov, L.K., Chukov, D.I., Kaloshkin, S.D., Kolesnikov, E., Nematulloev, S. (2020). The structural and mechanical properties of the UHMWPE films mixed with the PE-wax. Materials, 13(15): 3422. https://doi.org/10.3390/ma13153422

[25] Tenório Soares, I., de Muniz Almeida, C., de Maru Moraes, M.M., de Fátima Vieira Marques, M. (2022). Enhancement of mechanical properties of ultra-high molecular weight polyethylene nanocomposites without losing thermal stability. Journal of Applied Polymer Science, 139(28): e52618. https://doi.org/10.1002/app.52618

[26] Lebedev, O.V., Tikunova, E.P., Kurkin, T.S., Golubev, E.K., Ozerin, A.N. (2024). Nanocomposites based on disentangled ultra-high molecular weight polyethylene: Aspects and specifics of solid-state processing. Polymers, 16(23): 3423. https://doi.org/10.3390/polym16233423

[27] Chhetri, S., Bougherara, H. (2021). A comprehensive review on surface modification of UHMWPE fiber and interfacial properties. Composites Part A: Applied Science and Manufacturing, 140: 106146. https://doi.org/10.1016/j.compositesa.2020.106146

[28] Çelebi Efe, G., Yenilmez, E. (2022). Study on surface properties of UHMWPE/Hap composite coating on Ti6Al4V. Surface Engineering, 38(4): 417-429. https://doi.org/10.1080/02670844.2022.2077558

[29] Panin, S.V., Alexenko, V.O., Buslovich, D.G. (2022). High performance polymer composites: A role of transfer films in ensuring tribological properties—A review. Polymers, 14(5): 975. https://doi.org/10.3390/polym14050975

[30] Yellapragada, N.V.S.R., Madala, V.S.K., Devarakonda, S.K., Shaik, R.S.M.A., Annamdasu, N.R., Dasari, K.R., Mohammad, H.S. (2023). Application of Taguchi – PCA / GRA method to optimize the wear behaviour of polyester/carbon fibre composites. Revue des Composites et des Matériaux Avancés-Journal of Composite and Advanced Materials, 33(2): 65-73. https://doi.org/10.18280/rcma.330201

[31] Pillai, R.R., Mohan, L. (2025). Plasma surface modification of biomedical implants and devices: Emphasis on orthopedic, dental, and cardiovascular applications. Prosthesis, 7(6): 143. https://doi.org/10.3390/prosthesis7060143

[32] Yadav, M., Deshmukh, S.P. (2024). Tribological characterization and hardness analysis of acrylonitrile butadiene styrene composites reinforced with titanium dioxide and tungsten (ABS/TiO_2W). Revue des Composites et des Matériaux Avancés, 34(1): 19-25. https://doi.org/10.18280/rcma.340103

[33] Czwartos, J., Nowak-Stępniowska, A., Budner, B., Fok, T., Bartnik, A., Wachulak, P., Fiedorowicz, H. (2024). Polycaprolactone scaffold surface modification with soft X-ray/extreme ultraviolet (SXR/EUV) radiation and low-temperature oxygen and nitrogen plasma for biomedical applications. Journal of Materials Science, 59: 1193711951. https://doi.org/10.1007/s10853-024-09876-y

[34] Bhoi, S., Prasad, A., Kumar, A., Sarkar, R.B., Mahto, B., Meena, C.S., Pandey, C. (2022). Experimental study to evaluate the wear performance of UHMWPE and XLPE material for orthopedics application. Bioengineering, 9(11): 676. https://doi.org/10.3390/bioengineering9110676

[35] Nayak, S.K., Hirwani, J.K., Sinha, S.K., Pandey, R.K. (2024). Mechanical and bio-tribological behaviours of UHMWPE based composites for prosthetic hip joint implant application. Tribology International, 199: 109945. https://doi.org/10.1016/j.triboint.2024.109945

[36] de la Fuente-Jiménez, J.L., Rodríguez-Rivas, C.I., Mitre-Aguilar, I.B., Torres-Copado, A., et al. (2023). A comparative and critical analysis for in vitro cytotoxic evaluation of magneto-crystalline zinc ferrite nanoparticles using MTT, crystal violet, LDH, and apoptosis assay. International Journal of Molecular Sciences, 24(16): 12860. https://doi.org/10.3390/ijms241612860

[37] Rosa, V., Silikas, N., Yu, B., Dubey, N., et al. (2024). Guidance on the assessment of biocompatibility of biomaterials: Fundamentals and testing considerations. Dental Materials, 40(11): 1773-1785. https://doi.org/10.1016/j.dental.2024.07.020